

SUPPLEMENTAL FIGURES

Figure S1

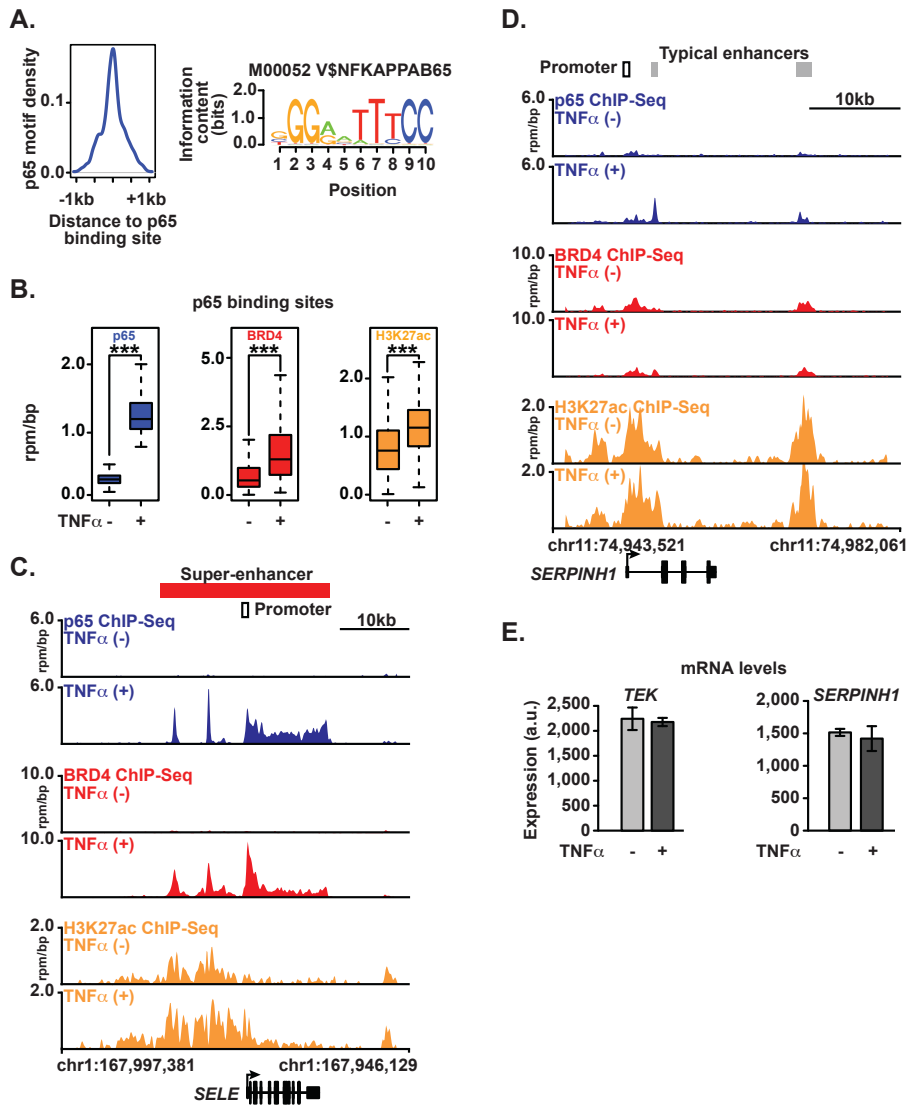


Figure S1 (related to Figure 1): p65 and BRD4 Genome Binding during Proinflammatory Activation in ECs

(A) Average density of p65 motifs in the +/- 1kb region flanking the center of all p65 binding sites measured by ChIP-Seq.

(B) Boxplot of p65, BRD4 and H3K27ac signal at all p65 binding sites in ECs before and after TNF α stimulation. ChIP-Seq signal is given in units of reads per million per base pair (rpm/bp). Significance of the difference between distributions determined using a two-tailed *t* test. *** p-value < 1e-10.

(C, D) Gene track of ChIP-Seq signal in units of rpm/bp for p65, BRD4 and H3K27ac at the *SELE* and *SERPINH1* loci.

(E) Bar plot of cell count normalized expression levels (arbitrary units) of *TEK* and *SERPINH1* in either untreated or TNF α (25 ng/mL, 3 hours) treated ECs. Data are represented as mean +/- SEM.

Figure S2

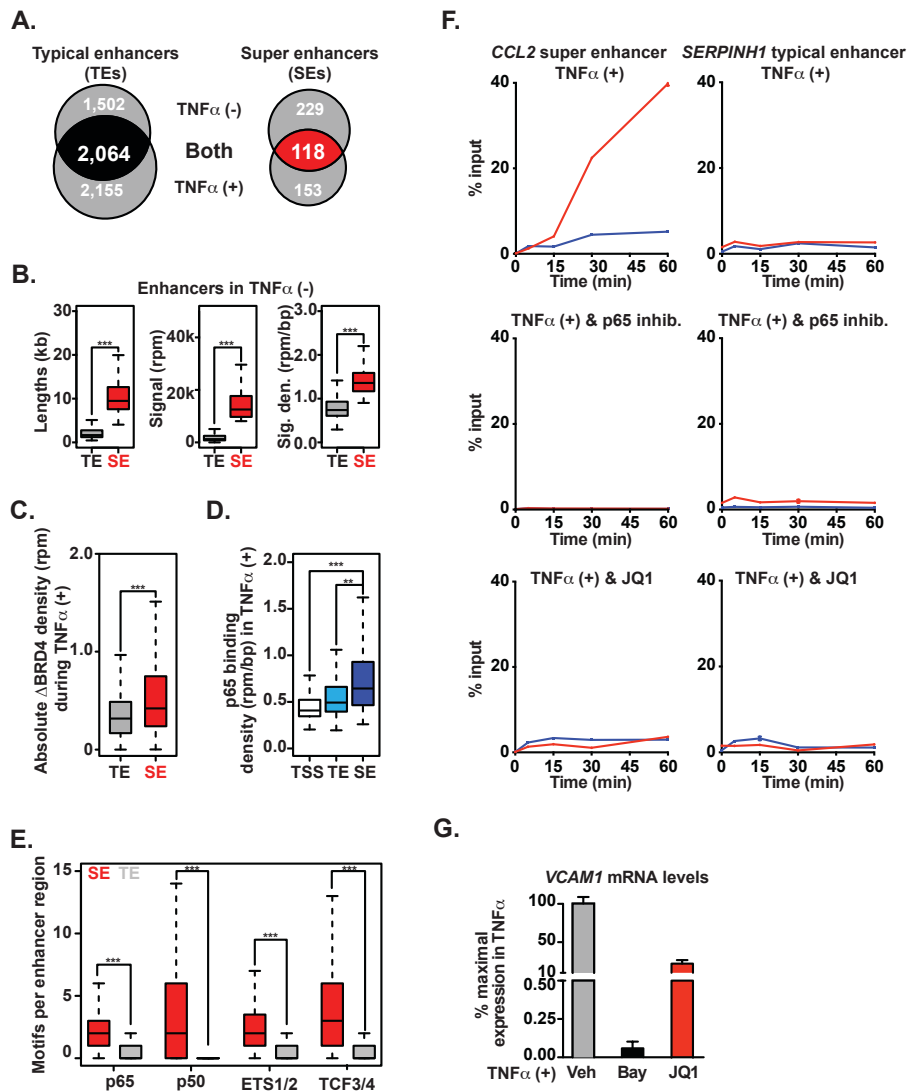


Figure S2 (related to Figure 2): p65 and BRD4 Establish Super Enhancers During Proinflammatory Stimulation

(A) Venn diagram of the total number of typical enhancer loci (left) and super enhancer loci (right) TNF α (-) and TNF α (+) treated ECs. The middle shaded area shows the number of conserved enhancers in both treatments.

(B) Boxplots of median enhancer DNA length (kb), signal (rpm) and signal density (rpm/bp) of TNF α -lost typical and super enhancer loci. Significance of the difference between distributions determined using a two-tailed *t* test. ** p-value < 1e-5, *** p-value < 1e-10.

(C) Boxplots of absolute change in BRD4 signal density at TNF α -gained typical enhancers compared to super enhancers. Significance of the difference between distributions determined using a two-tailed *t* test. ** p-value < 1e-5, *** p-value < 1e-10.

(D) Boxplots of absolute change in p65 binding density at transcriptional start sites of active genes, typical enhancers and super enhancers in TNF α (+) treated ECs. Significance of the difference between distributions determined using a two-tailed *t* test. ** p-value < 1e-5, *** p-value < 1e-10

(E) Boxplots of motif density at super enhancer regions (red) compared to typical enhancer regions (gray) in TNF α (+) treated ECs. Significance of the difference between distributions determined using a two-tailed *t* test. *** p-value < 1e-10.

(F) Line plots of kinetic ChIP-qPCR showing enrichment (% input) of p65 and BRD4 at an NF- κ B binding site in the *CCL2* (left) super enhancer and *SERPINH1* typical enhancer (right) in ECs treated with TNF α (25 ng/mL, 0, 5, 15, 30, 60 minutes). The effect of cotreatment with vehicle (top), BAY (NF-kB inhibitor, middle) and JQ1 is shown. Results are normalized to time 0. Data are represented as mean +/- SEM

(G) Bar plot of *VCAM1* mRNA levels measured by RT-qPCR in ECs treated with TNF α and co-treated with Vehicle, BAY (20 μ M) or JQ1 (500 nM). TNF α treatment was set to 100% and results displayed as percent reduction from TNF α alone. Data are represented as mean +/- SEM. Significance of the difference between distributions determined using a two-tailed *t* test. *** p-value < 1e-3

Figure S3

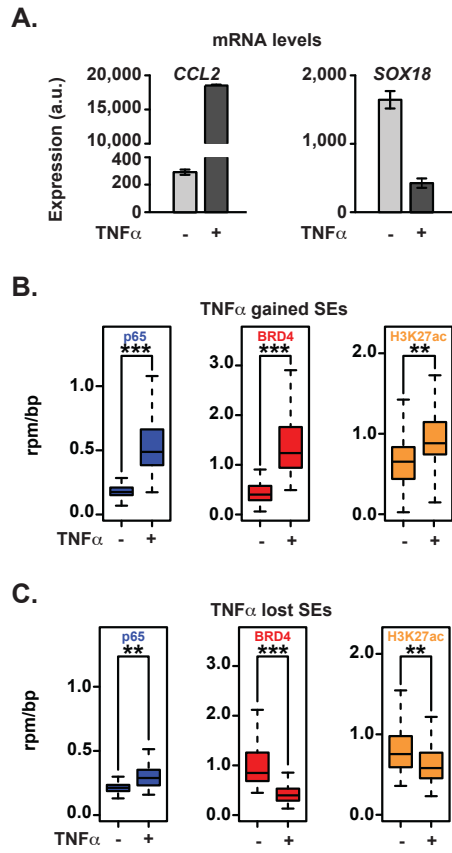


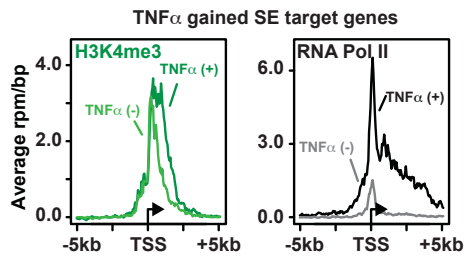
Figure S3 (related to Figure 3): NF- κ B Provokes Rapid, Global Redistribution of BRD4

(A) Bar plots of cell count normalized expression levels (arbitrary units) of the chemokine *CCL2* and the EC transcription factor *SOX18* in either untreated or TNF α (25 ng/mL, 3 hours) treated ECs. Error bars represent SEM.

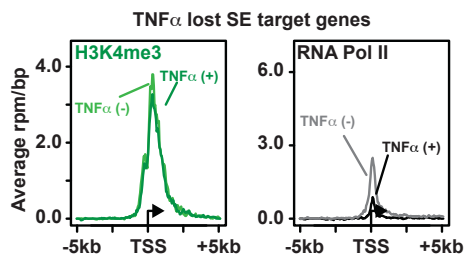
(B,C) Boxplots of p65, BRD4 and H3K27ac signal in units of rpm/bp at super-enhancers gained after TNF α treatment (B) or at super enhancers lost after TNF α treatment (C) in either TNF α untreated (left) or treated (right) cells. Significance of the difference between distributions determined using a two-tailed *t* test. ** p-value < 1e-5, *** p-value < 1e-10.

Figure S4

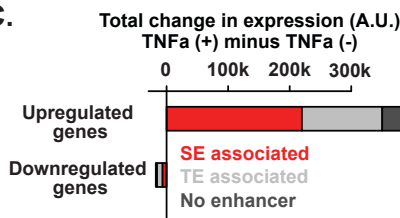
A.



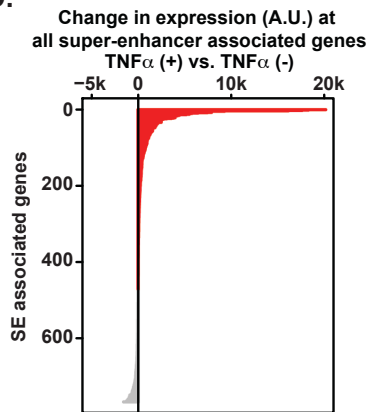
B.



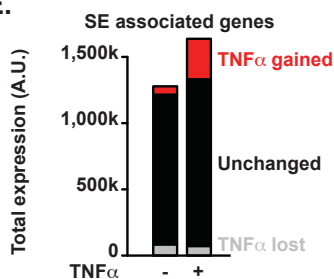
C.



D.



E.



F.

TNF α gained SE target genes (62 total)

Pathway	% List	FDR q value
KEGG_NOD_LIKE_RECEPTOR	6	<0.0001
KEGG_CYTOKINE_CYTOKINE_RECEPTOR	9	<0.0001
KEGG_CELL_ADHESION_MOLECULES	5	<0.0001
BIOCARTA_TGFB	3	<0.0001

G.

TNF α Lost SE target genes (110 total)

Pathway	% List	FDR q value
BIOCARTA_CELL2CELL_PATHWAY	4	<0.0001
KEGG_FOCAL_ADHESION	7	<0.0001
BIOCARTA_INTEGRIN_PATHWAY	4	<0.0001
KEGG_LEUKOCYTE_TRANSENDOTHELIAL_MIGRATION	4	<0.0005
BIOCARTA_VEGF_PATHWAY	2	0.004

H.

Conserved SE target genes (81 total)

Pathway	% List	FDR q value
PID_INTEGRIN3_PATHWAY	7	<0.0001
KEGG_ECM_RECEPTOR_INTERACTION	9	<0.0001
KEGG_FOCAL_ADHESION	9	<0.0001
REACTOME_HEMOSTASIS	11	<0.0001

Figure S4 (related to Figure 4): NF- κ B Formed Super enhancers Drive Proinflammatory Transcription

(A,B) H3K4me3 (green) and RNA Pol II (black) ChIP-Seq signal (rpm/bp) in the +/- 5kb region around the transcriptional start sites (TSS) of target genes that gain (A) or lose (B) super enhancers in response to TNF α . Light and Dark lines indicate signal in cells that are untreated or treated with TNF α respectively.

(C) Stacked bar graph showing the cumulative change in gene expression upon TNF α stimulation at genes with > 2 fold increase or decrease in gene expression (upregulated or downregulated genes). Cumulative changes in expression for genes proximal to super enhancers, typical enhancers, or no enhancer genes are plotted in red, light grey, and dark grey respectively. Units are in total increase or decrease in gene expression (A.U.) for all upregulated or downregulated genes respectively.

(D) Bar graph showing the absolute change in expression 3hrs post-TNF α stimulation for all genes associated with super enhancers in either TNF α (+) or TNF α (-) conditions. Change in expression is reported in absolute cell count normalized arbitrary units (A.U.). Genes are sorted by absolute change in expression between TNF α (+) and TNF α (-) with red and grey indicating upregulated and downregulated genes respectively.

(E) Stacked bar graph showing the contribution of TNF α (+) gained, TNF α (+) lost or unchanged super enhancer associated genes in TNF α (-) and TNF α (+) conditions. Cumulative expression of genes associated with TNF α (+) gained, TNF α (+) lost or unchanged super enhancer associated genes are shown as red, grey, or black bars respectively.

(F-H) Tables showing pathway enrichment of genes associated with TNF α -gained (F), TNF α -lost (G) and conserved (H) super enhancers using the Molecular Signatures Database (Broad Institute).

Figure S5

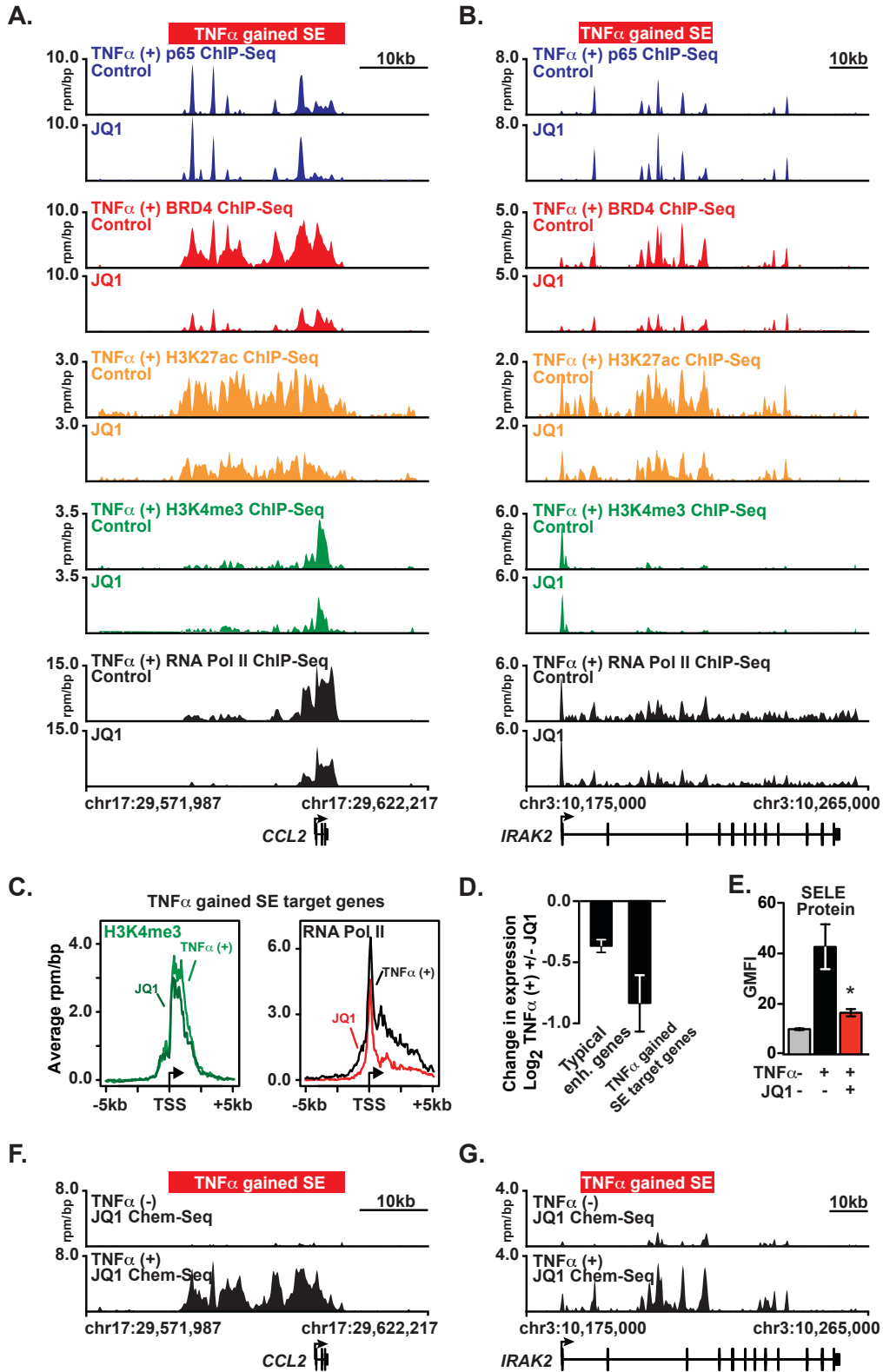


Figure S5 (related to Figure 5): NF- κ B Formed Super enhancers Drive Proinflammatory Gene Expression in a BET Bromodomain-Dependent Manner

(A,B) Gene tracks of ChIP-Seq signal in rpm/bp for p65, BRD4, H3K27ac, H3K4me3 and RNA Pol II at the *CCL2* (A) and *Irak2* (B) gene locus in ECs treated with TNF α in the absence (top) or presence (bottom) of JQ1. The x-axis depicts genomic position with the LPS gained super-enhancer shown as a box.

(C-) H3K4me3 (green) and RNA Pol II (black) ChIP-Seq signal (rpm/bp) in the +/- 5kb region around the transcriptional start sites (TSS) of target genes that gain super-enhancers in response to TNF α and in the presence or absence of JQ1. Light/dark green lines and black/red lines indicate the signal in cells that are untreated or treated with JQ1, respectively.

(D) Bar plots of the log₂ fold change in expression for genes associated with typical enhancers (left) or TNF α gained super enhancers (right) following TNF α stimulation and co-treatment with vehicle or JQ1. Error bars represent 95% confidence intervals of the mean.

(E) Bar plot of average gated mean fluorescence intensity (GMFI) of cell surface protein expression measured by FACs of E-selectin in ECs pretreated with JQ1 (500 nM, 3 hrs) followed by TNF α (25 ng/mL, 3 hrs). Error bars represent SEM. * p-value < .05 in JQ1 vs VEH.

(F, G) Chem-Seq tracks at the *CCL2* (F) and *IRAK2* (G) super enhancer locus in ECs from TNF α (-) and TNF α (+).

Figure S6

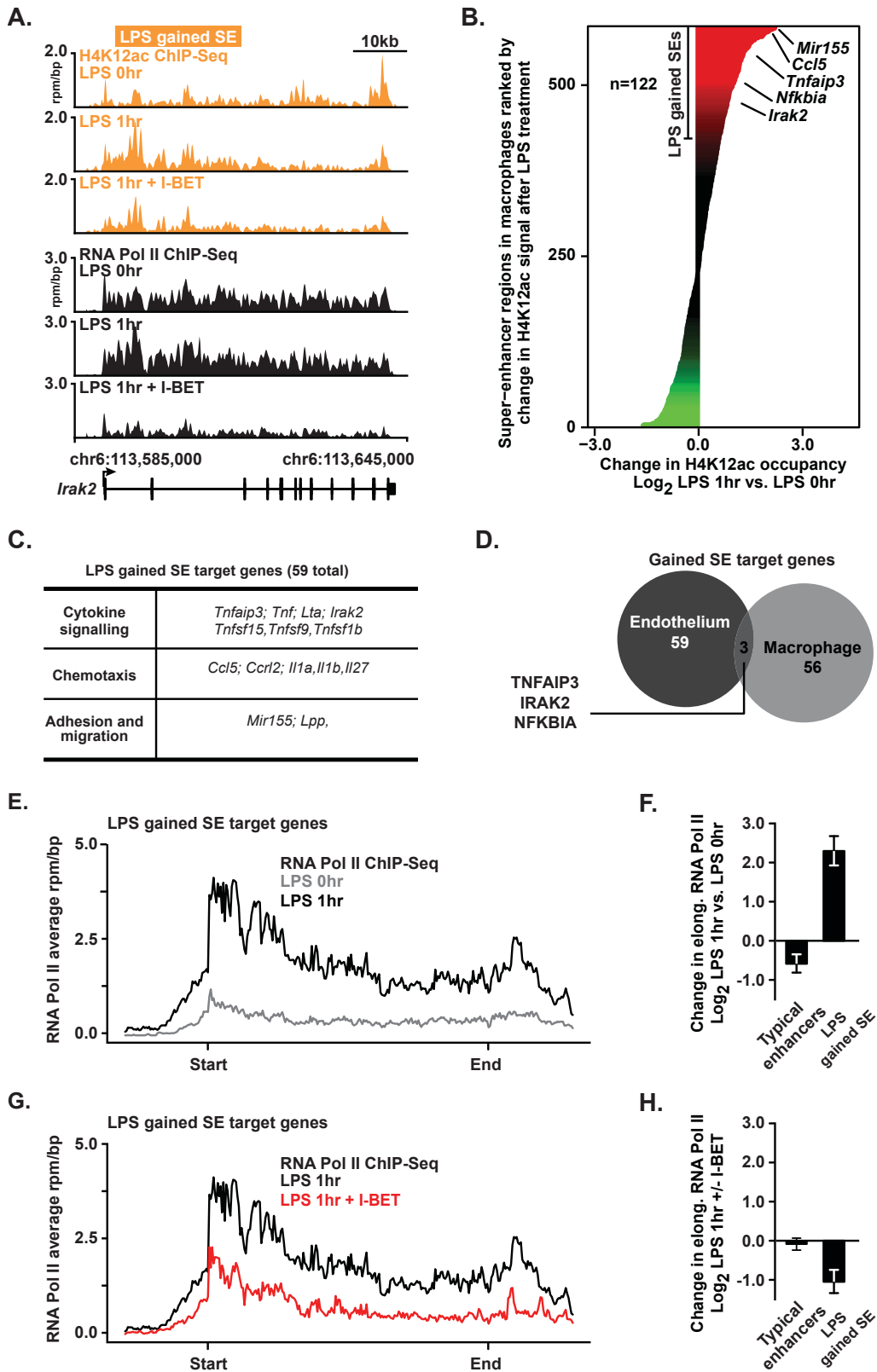


Figure S6 (related to Figure 5): BET Bromodomain Inhibition Disrupts Proinflammatory Super Enhancer Driven Transcription in Macrophages

(A) Gene tracks of ChIP-Seq signal in units of rpm/bp for H4K12ac and RNA Pol II at the *Irak2* in LPS treated mouse macrophages at either 0hr (top), 1hr (middle), or 1hr + I-BET (bottom). The x-axis depicts genomic position with LPS gained super enhancers shown as orange boxes.

(B) All genomic regions containing a super enhancer in 0hr or 1hr LPS treated macrophages are shown ranked by \log_2 change in H4K12ac signal (1hr vs. 0hr). X-axis shows the \log_2 fold change in H4K12ac signal. Super enhancers with a greater than 2 fold change in H4K12ac signal are colored red (2 fold gain) or green (2 fold loss).

(C) Table showing functional classification of genes associated with super-enhancers gained after LPS stimulation in primary BMDM.

(D) Venn diagram displaying the number of either $\text{TNF}\alpha$ or LPS gained super-enhancer associated genes in endothelium and macrophages respectively. Genes that overlap in the two cell types are listed.

(E,G) Metagene representations of average RNA Pol II ChIP-Seq signal in units of rpm/bp at a meta composite of target genes of super enhancers that are gained in response to LPS treatment. (E) RNA Pol II signal in 0hr and 1hr LPS treated macrophages are depicted in gray or black lines respectively. (G) RNA Pol II signal in 1hr LPS control and I-BET treated macrophages are depicted in black or red lines respectively.

(F,H) Bar plots of the \log_2 fold change in RNA Pol II ChIP-Seq for genes associated with typical enhancers (left) or target genes of $\text{TNF}\alpha$ gained super enhancers (right). (E) shows the \log_2 fold change between 1hr and 0hr LPS treatment. (F) shows the \log_2 fold change in 1hr LPS treated macrophages between I-BET and control co-treated cells. Error bars represent 95% confidence intervals of the mean.

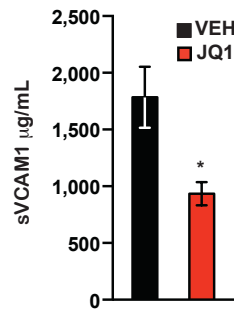
Figure S7

A.

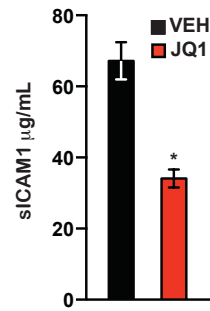
Treatment	No. of mice	No. of vessels	WBC ($10^3/\mu\text{l}$)	Vessel diam. (μm)	Shear rate (s^{-1})
VEH + TNF α	5	22	5.8 ± 0.27	26.8 ± 1.0	1044 ± 49
JQ1 + TNF α	5	25	5.4 ± 0.47	27.5 ± 1.0	986 ± 36

Values are mean \pm sem

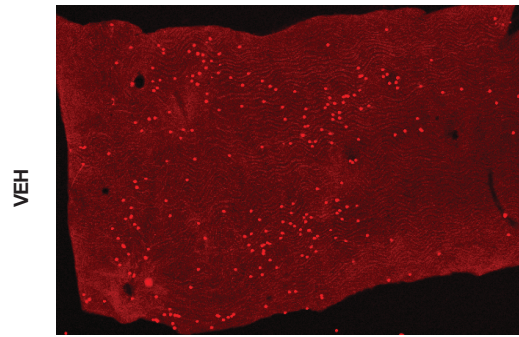
B.



C.



D.



E.

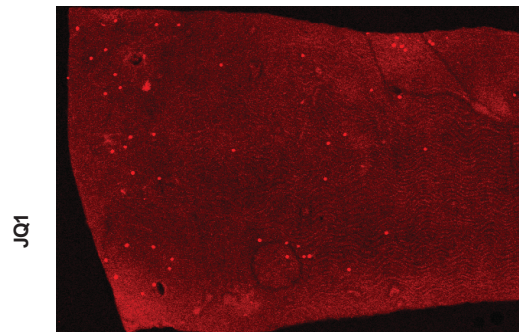
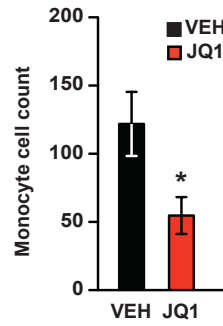


Figure S7 (related to Figure 7): BET Bromodomain Inhibition Attenuates Atherogenesis in LDLr^{-/-} Model

(A) Table of physiologic parameters of mice studied during intravital microscopy leukocyte rolling experiment.

(B,C) Bar plots showing the mean effect of JQ1 on circulating soluble VCAM1 levels (A) and soluble ICAM1 levels (B) in Ldlr^{-/-} animals. Levels are measured in units of circulating µg/ml. Data are represented as mean +/- SEM. Significance determined using a two-tailed *t* test. * p-value < .05.

(D) Image showing the adhesion of fluorescently labeled, unstimulated monocytes (U937 cells) on aortas isolated from Ldlr^{-/-} animals maintained on atherogenic diet (6wks) while treated with vehicle or JQ1 (50 mg/kg).

(E) Bar plot quantifying mean monocyte adhesion in *ex vivo* aortic adhesion assay. Units are in cell counts per low power field. Data are represented as mean +/- SEM. Significance determined using a two-tailed *t* test. * p-value < .05 in JQ1 vs. VEH.

SUPPLEMENTAL DATA TABLES

File S1: Datasets and backgrounds

Table listing the names and GEO accession numbers for all ChIP-Seq datasets generated or analyzed in this study. If applicable, the background dataset used in enriched region analysis is provided.

File S2: Human EC super enhancers .bed file

.bed format file (genome.ucsc.edu/FAQ/FAQformat.html#format1) containing the genomic coordinates for all super-enhancers (determined by BRD4 ChIP-Seq occupancy) in endothelial cells (ECs). Coordinates are in genome build HG18. Individual tracks are provided for super enhancers conserved in both untreated and TNF α treated conditions (black), those gained in response to TNF α treatment (red), and those lost in response to TNF α treatment.

File S3: Target genes of super enhancers gained or lost in response to TNF α treatment in ECs

List of all candidate target genes of super enhancers that are either gained or lost in response to TNF α treatment in ECs.

File S4: Mouse macrophage super enhancers .bed file

.bed format file (genome.ucsc.edu/FAQ/FAQformat.html#format1) containing the genomic coordinates for all super enhancers (determined by H4K12ac ChIP-Seq occupancy) in mouse macrophages. Coordinates are in genome build MM9. Individual tracks are provided for super enhancers conserved in 0hr and 1hr LPS treated conditions (black), those gained in response to 1hr LPS treatment (red), and those found in 0hr LPS treatment that are lost after 1hr (green).

File S5: Target genes of super enhancers gained in response to LPS in mouse macrophages

List of all candidate target genes of super enhancers that are either gained or lost in response to 1hr LPS treatment in mouse macrophages.

EXTENDED EXPERIMENTAL METHODS

RNA isolation, reverse transcription and real-time PCR. Total cellular mRNA was isolated using an RNeasy kit (Qiagen). Following isolation, 500 ng of RNA was digested with DNase (Invitrogen) and reverse transcribed using QuantiTect kit (Qiagen). Real Time PCR (RT-PCR) was performed in a MyiQ Single-Color Real Time PCR system using SYBR Green I (Bio-Rad). The mRNA levels of test genes were normalized to the 36B4 internal control gene and fold change calculated by the $\Delta\Delta C_t$ method. Primers for RT-PCR are provided upon request.

NF- κ B Inhibition Effect on VCAM1 Expression. HUVEC were cultured in growth conditions as above. Cells were pretreated with Vehicle, BAY 11-7082 (20 μ M, Sigma-Aldrich) or JQ1 (500 nM) for 1hr then stimulated with TNF α (10 ng/mL, 3 hours). Total cellular mRNA was isolated, reverse transcribed, RT-PCR was performed and the mRNA levels of VCAM1 were normalized to 36B4 internal control gene. Fold change from maximal stimulation was calculated by the $\Delta\Delta C_t$ method, setting TNF α treated samples to 100%.

JQ1 Concentration Effect on Gene Expression. HUVEC cultured in growth conditions were pretreated with JQ1 (50, 100, 250, 500 nM) for 1hr prior to treatment with TNF α (10 ng/mL, 3 hours). Total cellular mRNA was isolated, reverse transcribed and RT-PCR performed for test genes normalized to 36B4 internal control gene. Fold change from maximal stimulation was calculated by the $\Delta\Delta C_t$ method, setting TNF α treated samples to 100%.

RNA isolation and spike-in addition for cell count normalized microarray expression. Total cellular RNA was isolated using the miRNeasy kit (Qiagen) as per protocol. During isolation, external RNA spike-ins (ERCC, Ambion) were added at the time of cell lysis (Loven et al., 2012). For spike-in a 1:10 dilution of the concentrated RNA stock was made and one microliter of this working stock was added to 4x10⁶ cells.

RNA cell count microarray expression analysis. Microarray expression data were normalized as in (Loven et al., 2012) to produce cell count normalized expression values in arbitrary units. Expression data can be found at GSE53999.

Immunoblotting. HUVEC were grown in 12 well plates and lysed in RIPA buffer containing EDTA and protease inhibitors (Roche). Following SDS-PAGE separation on 3-8% Tris Acetate gels (Invitrogen), immunoblotting was performed using antibodies to BRD4 (Bethyl Laboratories), p65 (Santa Cruz), Tubulin (Santa Cruz) or Ku-70 (Santa Cruz) as described previously (Anand et al., 2013).

siRNA transfection. HUVEC monolayers were transfected with siRNA constructs (Ambion) using siDeliverX reagent (Panomics) per manufacturer's protocol (siRNA 30 nM). Protein knockdown was assessed 48 hours after transfection and experiments with TNF α stimulation were started at this point.

Flow cytometry, and CXCL8 quantification. HUVEC treated with JQ1 (500nM, 3 hours) followed by TNF α (10ng/mL, 3 hours) were harvested with cell dissociation buffer (Sigma-Aldrich), washed with cold PBS and fixed (1% paraformaldehyde, 30 min, 4°C). Cells were washed with cold PBS, centrifuged and incubated with 50 μ l of hybridoma supernatant containing mouse anti-human primary antibodies: ICAM1 (HU5/3), VCAM1 (E1/6), E-selectin (H4/18), and CD105 (E1/1), secondary staining done with a FITC-conjugated goat anti-mouse antibody (Poly453, 5 μ g/ml) from Biolegend (San Diego, CA). All data were acquired on a FACSCalibur flow cytometer (BD Biosciences, San Jose, CA) and analyzed with FlowJo 9.3.1 software (TreeStar, Inc.). For CXCL8 quantification, supernatants from treated ECs were harvested and analyzed with electrochemiluminescence detection system per manufacturer protocol (Meso Scale Discovery, Gaithersburg, MD).

Chromatin immunoprecipitation (ChIP). HUVEC were grown to confluence in 15 cm plates (1×10^7 cells), treated with JQ1 for 3 hours, followed by TNF α (25 ng/mL, 1 hour) in growth medium. Cells were cross-linked with 1% formaldehyde (10 minutes) followed by quenching (125 mM glycine). Cells were washed in cold PBS and harvested by cell scraper in cold PBS with protease inhibitors (Roche). Cells were centrifuged at 1650 x g for 5 minutes. Pellets were resuspended in cytosolic then nuclear lysis buffer and DNA was sheared on ice using a waterbath sonicator (Bioruptor, Diagenode) for 15 minutes at high output (30" on, 30" off) in 1mL of sonication buffer, as previously described (Rahl et al., 2010). Antibodies for ChIP: BRD4 (Bethyl A301-985A), p65 (Santa Cruz, sc-372X), RNA polymerase II (Santa Cruz sc-899), H3K27ac (Abcam, ab4729), H3K4me3 (Abcam, ab8580). For ChIP, 5 μ g of antibody was used for each IP.

Kinetic Chromatin Immunoprecipitation. HUVEC were grown to confluence as above for ChIP and pretreated with Vehicle, BAY 11-7082 (20 μ M), JQ1 (500 nM) or BAY + JQ1 for 1 hr then stimulated with TNF α , (10 ng/mL) for indicated time points. Cells were harvested ChIP performed as detailed above. Following DNA purification, qRT-PCR was performed with primers that amplify the most prominent NF-kB binding site in the *VCAM1* and *CCL2* 5' super enhancer or the 5' typical enhancer site for *TEK* and *SERPINH1*.

Chem-Seq. HUVEC were grown as above for ChIP and stimulated with TNF α (25 ng/mL, 1 hr). After cross-linking in formaldehyde, quenching with glycine and cell lysis and DNA sonication, chromatin was immunoprecipitated with the biotinylated-JQ1 compound (10 μ M), with free biotin (Sigma-Aldrich) serving as a negative control (Anders et al., 2014). Remainder of purification and sequencing was the same as described for ChIP.

Illumina DNA Sequencing and Library Generation. Purified ChIP DNA was used to prepare Illumina multiplexed sequencing libraries. Libraries for Illumina sequencing were prepared following the Illumina TruSeqTM DNA Sample Preparation v2 kit protocol with the following exceptions. After end-repair and A-tailing, immunoprecipitated DNA (~10-50ng) or whole cell extract DNA (50ng) was ligated to a 1:50 dilution of Illumina Adapter Oligo Mix assigning one of 24 unique indexes in the kit to each sample. Following ligation, libraries were amplified by 18 cycles of PCR using the HiFi NGS Library Amplification kit from KAPA Biosystems. Amplified libraries were then size-selected using a 2% gel cassette in the Pippin PrepTM system from Sage Science set to capture fragments between 200 and 400 bp. Libraries were quantified by qPCR using the KAPA Biosystems Illumina Library Quantification kit according to kit protocols. Libraries with distinct TruSeq indexes were multiplexed by mixing at equimolar ratios and running together in a lane on the Illumina HiSeq 2000 for 40 bases in single read mode.

ChIP-Seq Data analysis

Accessing data generated in this manuscript. All ChIP-Seq and Chem-Seq data generated in this publication can be found online associated with GEO Publication Reference ID GSE53998 (www.ncbi.nlm.nih.gov/geo/). This Publication Reference ID also includes the microarray data. GEO accession numbers for all analyzed datasets can also be found in File S1. Aligned and raw data can be found online associated with the GEO Accession ID GSE54000.

Gene sets and annotations. All analysis was performed using RefSeq (NCBI36/HG18) human gene annotations or RefSeq (NCBI37/MM9) mouse gene annotations.

ChIP-Seq and Chem-Seq data processing. All ChIP-Seq and Chem-Seq datasets were aligned using Bowtie (version 1.0.0) to build version NCBI36/HG18 of the human genome or build version NCB37/MM9 of the mouse genome (Langmead et al., 2009). Alignments were performed using the following criteria: -n2, -e70, -m1, -k1, --best. These criteria preserved only reads that mapped uniquely to the genome with 1 or fewer mismatches.

Calculating read density. We calculated the normalized read density of a ChIP-Seq or Chem-Seq dataset in any region as in (Lin et al., 2012). Briefly, ChIP-Seq reads aligning to the region were extended by 200bp and the density of reads per basepair (bp) was calculated. The density of reads in each region was normalized to the total number of million mapped reads producing read density in units of reads per million mapped reads per bp (rpm/bp).

Identifying ChIP-Seq and Chem-Seq enriched regions. We used the MACS version 1.4.2 (Model based analysis of ChIP-Seq) (Zhang et al., 2008) peak finding algorithm to identify regions of ChIP-Seq enrichment over background. A p-value threshold of enrichment of $1e-9$ was used for all datasets. The GEO accession number and background used for each dataset can be found in the accompanying supplementary File S1.

Identifying transcriptionally active genes. Genes were considered transcriptionally active if an RNA Pol II enriched region overlapped the TSS \pm 1kb promoter proximal region in either resting or TNF α treated ECs.

Determining genomic localization of p65 binding sites. The genomic localization of p65 ChIP-Seq enriched regions in TNF α treated ECs was determined using the CEAS software (Shin et al., 2009). Promoter regions were defined as \pm 5kb from the transcription start site (TSS). Gene body regions were defined as all regions contained inside annotated RefSeq transcripts outside of the promoter region. Intergenic regions were defined as all other regions in the genome (Figure 1E).

Creating heatmap representations of ChIP-Seq occupancy. Heatmaps of ChIP-Seq occupancy for various factors were created as in (Lin et al., 2012). Heatmaps were created for the \sim 6,000 p65 binding enriched regions. Each row plots the \pm 5kb region

flanking the center of the p65 enriched region. Rows are ranked by peak occupancy of p65 in TNF α treated ECs (Figure 1F).

Determining p65 motif density. p65 motif density was calculated in p65 ChIP-Seq enriched regions using the p65 (RelA) binding motif GGGRATTTCC (Transfac motif M00052) (Kunsch et al., 1992; Matys et al., 2006). The density of motifs was plotted relative to the +/-1kb region from the center of all p65 ChIP-Seq enriched regions (Figure S1A).

Mapping enhancers and super enhancers. Enhancers and super enhancers were mapped using the ROSE software package described in (Loven et al., 2013; Whyte et al., 2013) and available at (younglab.wi.mit.edu/super_enhancer_code.html). In ECs, BRD4 ChIP-Seq enriched regions in either control or TNF α treated conditions were used to map enhancers and super enhancers. In mouse macrophages, ChIP-Seq enriched regions for the enhancer associated H4K12ac mark in either 0hr or 1hr LPS stimulated cells were used to map enhancers and super enhancers. H4K12ac was used as a surrogate mark for enhancers as its genomic localization correlates with enhancer activity. It and other histone acetyl marks can be used to map super enhancers (Hnisz et al., 2013; Whyte et al., 2013).

Statistics of super-enhancers and typical enhancers. For typical and super-enhancers mapped with BRD4 ChIP-Seq in TNF α +/- conditions, enhancer lengths, BRD4 binding signal, and BRD4 binding density were calculated and displayed either as a fraction of the enhancer total (Figure 2B) or as a box plot (Figure 2C; Figure S2B). To quantify changes in typical or super-enhancer regions during TNF α stimulation, the set of all regions considered a typical enhancer in either TNF α +/- were enumerated, as was the set of all regions considered a super-enhancer in either TNF α +/- . Regions that were typical enhancers in one condition, but super-enhancers in the other were not considered part of the typical enhancer set. For each enhancer, the absolute change in BRD4 signal or density +/- TNF α was quantified and compared between typical-enhancers and super-enhancers (Figure 2D; Figure S2C). The statistical significance of differences between distributions of enhancer attributes between typical and super-enhancers in TNF α +/- conditions was assessed using a Welch's two-tailed *t* test.

Quantifying p65 binding at regulatory regions in TNF α treated ECs. p65 binding signal or density was quantified at all super-enhancers, typical-enhancers, and promoters of transcriptionally active genes in TNF α treated ECs (Figure 2E; Figure S2D). The

statistical significance of differences between distributions of p65 was assessed using a Welch's two-tailed *t* test.

Motif occupancy at super-enhancers and typical enhancers. Motif densities of NF- κ B, WNT, and ETS family transcription factors were determined at BRD4 defined enhancer regions in TNF α treated ECs. For each enhancer region, the search space was restricted to regions in H3K27ac valleys (see below). Motif densities were calculated using position weight matrices for p50, p65, TCF3/4, and ETS1/2 derived from Transfac, (Transfac motifs M00194, M00052, M02816, M03977 respectively) (Matys et al., 2006). For each transcription factor, sequence space was scanned for high-probability motif occurrences compared to a background of scrambled sequence. Motifs underlying enhancer regions are displayed in Figure 2F and 2G, and quantified at all super-enhancer and typical enhancers in Figure S2E. The statistical significance of differences between distributions of p65 was assessed using a Welch's two-tailed *t* test.

Identifying candidate transcription factor binding regions from H3K27ac valleys. Regions between peaks of H3K27ac have been shown to harbor transcription factor binding sites (Gerstein et al., 2012). To identify these regions, we first defined the valleys in each enhancer region as described in (Ramsey et al., 2010). 10 bp bins were assigned a valley score, then adjacent bins were stitched and their sequence was extended 100 bp on either side to search for transcription factor binding motifs

Identifying TNF α gained/lost super-enhancers. In order to quantify changes in super-enhancers between two conditions, background subtracted ChIP-Seq signal was calculated at the set of all enhancer regions considered super in at least one condition. Gained/lost super-enhancers were determined as those with a greater than 2 fold change signal in either direction. In ECs, changes in super-enhancers were determined by comparing BRD4 signal between control untreated and TNF α treated cells (Figure 3C). In mouse macrophages, changes in super-enhancers were determined by comparing H4K12ac signal between 0hr and 1hr LPS stimulated cells (Figure S6B).

Correlating p65 occupancy with BRD4 change at TNF α gained/lost super-enhancers In order to quantify binding of p65 in relation to change in BRD4 at super enhancers, all super enhancers in either TNF α (-) or TNF α (+) conditions were ranked by change in BRD4. Super enhancers were then binned (50/bin) and the median p65 background subtracted ChIP-Seq occupancy at super enhancers was calculated. To determine 95%

confidence intervals, the median was resampled with replacement 1000 times (Figure 3D).

Comparing transcription factor motif densities at TNF α gained/lost super-enhancers. Transcription factor motif densities were calculated at TNF α gained and lost super-enhancer regions for 642 motifs with annotated PWMs (Matys et al., 2006). Motif instances were calculated as before to generate observed counts. To generate expected motif background frequencies, TNF α gained and lost super-enhancers regions were respectively scrambled to maintain dinucleotide frequencies akin to the actual genomic sequences. Motifs were considered present in these regions if they had an observed/expected ratio > 1.5 fold in either TNF α gained or lost super-enhancer regions. For all 21 detected motifs, the log₂ ratio of observed frequencies between TNF α gained and lost super-enhancers was calculated and plotted ranked by decreasing gained vs. expected ratio (top to bottom) (Figure 3E).

Quantifying elongating RNA Pol II density in gene body regions. Elongating RNA Pol II density was defined as the density of RNA Pol II in the +300 bp TSS to +3,000bp gene end region which roughly corresponds to the gene body extending past the RNA Pol II initiation promoter region and ends at the RNA Pol II transcription termination region (Rahl et al., 2010).

Quantifying changes in transcription and gene expression of TNF α gained/lost super-enhancer proximal genes. Genes within 100kb of super-enhancer and typical enhancer regions in TNF α +/- were first identified and filtered for transcriptional activity (as above), or for expression (> 100 A.U. expression in either TNF α +/- conditions). Genes were then assigned to gained/lost/conserved super-enhancers (as defined above), or to gained/lost/conserved typical enhancers (using the same criteria to define gain/loss). Genes proximal to both a super-enhancer and a typical enhancer were assigned to super-enhancers. Transcriptionally active and expressed genes without proximal enhancers (within 100kb) were labeled “no enhancer genes”. At each cohort of genes, the log₂ change in elongating RNA Pol II density or mRNA expression upon TNF α stimulation was calculated and the mean change was plotted (Figure 4A,B). 95% confidence intervals of the mean were determined through empirical resampling with replacement (10,000 iterations). The statistical significance of differences between distributions of changes was also assessed using a Welch’s two-tailed *t* test.

Correlating changes in BRD4 at super enhancers to changes in transcription and expression at proximal genes. Super enhancers found in either TNF α (-) or TNF α (+) conditions were ranked by their change in BRD4 as calculated previously. For each super enhancer, proximal active genes (TSS within 50kb of the super enhancer) were identified. The change in either gene body elongating RNA Pol II or mRNA levels at these genes was calculated and plotted relative to change in BRD4 (Figure 3C,E). To reduce noise in the visualization, median change in either elongating RNA Pol II or mRNA was plotted in 50 binned intervals evenly distributed across ranked genes. A loess fit was overlaid on plots to capture overall trends.

Identifying target genes of gained/loss super-enhancers. Candidate target genes of gained or lost super-enhancers were determined by identifying nearby genes whose TSS was found within 100kb of the super enhancer center. We next examined the promoter (+/- 1kb TSS) region of these genes for changes in ChIP-Seq factor occupancy as evidence for regulation by proximal super enhancers. For gene targets of TNF α gained super enhancers, candidate genes with at least 1.5 fold increases in BRD4 and p65 were considered targets (Figure 4). Conversely, candidate genes within 100kb of TNF α lost super enhancers were considered targets if a 1.5 fold or greater loss in BRD4 was observed at promoters (Figure 4). In mouse macrophages, targets of LPS gained super enhancers were determined as those within 100kb that had at least a 1.5 fold gain in H4K12ac at their promoters (Figure S6).

Creating meta-gene representations of ChIP-Seq occupancy. Meta-gene representations of RNA Pol II and H3K4me3 density (Figure 4,5 and Figure S4-6) were determined by first binning gene sets into three regions: i) the upstream promoter - from 3kb upstream of the TSS to the TSS (50bp bins), ii) the gene body - from the TSS to the gene end (200 bins), iii) the transcription termination region (TTR) - from the gene end to +3kb downstream (50bp bins). ChIP-Seq density in each region was calculated and the average density in that region was plotted in units of average rpm/bp. Meta-gene representations in TSS regions were calculated similarly by binning the +/-5kb tss region into 50bp bins (Figure 4,5 and Figure S6). The differences in relative ChIP-Seq density in gene regions were tested for statistical significance using a Welch's two-tailed *t* test.

Quantifying changes in chromatin occupancy at typical enhancers vs. super enhancers and their associated genes. For various comparisons, log₂ change in ChIP-Seq occupancy was calculated at typical enhancers or super enhancers. To test the

statistical significance of changes between typical enhancers and super enhancers, we utilized empirical resampling with replacement to identify 95% confidence intervals of the mean change (Figure 5B). A similar method was used to calculate changes in ChIP-Seq occupancy or gene expression at genes associated with typical enhancers or gained/lost super enhancer target genes (Figure S5D,S6F,S6H).

Correlating JQ1 genomic binding via Chem-Seq to changes in BRD4 and H3K27ac occupancy. JQ1 genomic binding was calculated at regions of JQ1 Chem-Seq enrichment in TNF α stimulated conditions and plotted against the log₂ change in BRD4 or H3K27ac upon JQ1 treatment (Figure 5F and 5G). A loess fit line was added to the scatter plot distribution to capture overall trend (black line). The Pearson correlation between JQ1 genomic occupancy and BRD4 or H3K27ac change is provided.

Intravital microscopy. 8 week old, male, C57Bl/6 mice (n=5/group) were pre-anesthetized with 90-200 mg/kg ketamine/10 mg/kg xylazine. Animals were pretreated with JQ1 (50 mg/kg) at 15 hours and 1 hour prior to TNF α treatment. Inflammation was induced by intrascrotal injection TNF α (200 ng, 100 μ l volume) and the cremaster muscle was exteriorized 2 hours later. The cremaster vessel was perfused with thermocontrolled (37C) and aerated (5% CO₂, 95% N₂) bicarbonate-buffered saline. Microvessel data were obtained using a confocal intravital microscope (Olympus FV 1000) with a 40x water immersion objective. Leukocyte rolling in the venules was recorded for 60s using a digital video camera connected to an IBM-compatible computer. The centerline red blood cell velocity (V_{cl}) in each venule was measured in real time with a dual photodiode velocimeter. Systemic leukocyte counts were calculated from a 50 μ l, retroorbital blood sample taken at the completion of the experiment. After the start of the cremaster surgery, data was acquired for 30 min in 5-8 separate vessels, then mice were euthanized.

Video recordings from the intravital microscopy experiments were analyzed off-line on a computer based image acquisition system, and vessel diameter determined using NIH Image J software. The centerline red cell velocity recorded from each vessel was used to determine the volumetric blood flow (Q) via the equation $Q = (V_{cl})(0.625)(A_{cs})$, where A_{cs} is the cross-sectional area of the cylindrical vessel, and 0.625 is an empirical correction factor. For each vessel, wall shear rate (W_{sr}) was also determined: $W_{sr}=2.133[(8 \times 0.625 \times V_{cl})/D_v]$, where D_v is the vessel diameter. Critical velocity (V_{crit}) is also calculated: $V_{crit}=(V_{cl} \times 0.625)(D_{cell}/D_v)[(2 - (D_{cell}/D_v))]$. Recordings of each vessel were

analyzed for 30–60 s, and rolling leukocytes, primarily neutrophils, were identified as the visible cells passing through a plane perpendicular to the vessel axis. Rolling leukocyte flux is defined as the total number of cells passing through a plane perpendicular to the vessel axis per minute. To compensate for differences in systemic leukocyte count between mice, leukocyte rolling flux was also represented as the leukocyte rolling flux percent, which is defined as the rolling leukocyte flux divided by the product of the systemic leukocyte count and the volumetric blood flow (Q) through the vessel per minute.

Cell adhesion assay. HUVECs were plated onto 96-well fluorescence plates (353948; BD). The following day, cells were pretreated with JQ1 (500 nM, 1 hour) followed by TNF α (10 ng/ml, 5 hours). THP-1 cells (ATCC) were washed with serum-free RPMI 1640 and suspended at 5×10^6 cells/mL in medium with Calcein AM (5 μ M, C3100MP; Invitrogen). Incubated at 37°C, 5% CO₂ for 30 minutes. The labeling reaction was stopped by addition of growth medium. Cells were washed with growth medium twice and resuspended in growth medium at 5×10^5 cells/mL. TNF α treatment (5 hours) HUVECs were washed once with THP-1 growth medium, and 200 μ l Calcein AM–loaded THP-1 cells were added to each well. After 1 hour of incubation, nonadherent cells were removed. Cells were gently washed with prewarmed RPMI 1640 medium 4-6 times. Fluorescence was measured by using a fluorescence plate reader at 485 nm excitation. For siRNA experiments, HUVEC were transfected with siRNA in 12 well plate. 48 hours after transfection, HUVEC were replated into 96 well plates and assay performed as above.

Leukocyte-endothelial transmigration assays. HUVEC (subculture 2) pretreated with vehicle or JQ1 (1 hour) were grown on fibronectin-coated glass before insertion into the flow chamber for transmigration assays at 37°C. Freshly isolated (untreated) neutrophils were resuspended in 10^6 cells/mL in DPBS containing 0.2% (v/v) HSA and 20mM HEPES, pH 7.4 and then drawn through the chamber at a constant rate of 0.85 ml/min (estimated shear stress – 1.8 dynes/cm²). Neutrophil adhesion and transmigration were determined after 10 minutes of perfusion by analysis of six high power fields (x20) as described (Yang et al., 2005).

Aortic adhesion assay (ex vivo). LDL receptor knockout mice (N= 10, 4 week old, female) on a C57Bl/6 background (Jackson Laboratories) were fed an atherogenic diet for 6 weeks. Animals were also treated with vehicle (DMSO) or JQ1 (50 mg/kg) by intraperitoneal injection, once daily, starting four days after initiation of the atherogenic

diet. JQ1 was prepared as previously described (Filippakopoulos et al., 2010). At the end of 6 weeks on diet, animals were euthanized with CO₂ and perfused with 10 mL of sterile PBS. Aortas were excised intact from animals and maintained in RPMI media supplemented with 10% FBS, penicillin/streptomycin antibiotics and either 0.1% DMSO or JQ1 500nM. After excision, aortas were opened longitudinally and pinned on sterile agarose plates and maintained in RPMI media until the time of monocyte adhesion (between 2-5 hours). U937 monocytes were labeled with cell tracker orange (Molecular Probes) per manufacturer protocol and resuspended in RPMI with 10% FBS at a concentration of 1.25×10^5 /mL. Aortas were incubated for 30 minutes with 2.5×10^5 cells in 2 mL of media at 37°. After incubation, aortas were washed 6 times with sterile PBS and then fixed overnight in 10% neutral buffered formalin. The following day, aortas were coverslipped on a slide and images were taken using confocal microscope (Olympus FV 1000). Images were acquired with 4x objective and cells were counted in 2 separate low power field of views using image J software.

Human neutrophil isolation. Human neutrophils were isolated from anticoagulated whole blood of healthy volunteers as previously described (Yang et al., 2005). Leukocytes were separated from whole blood by Ficoll-Hypaque density gradient ultracentrifugation. Neutrophils were further purified by dextran sedimentation and hypotonic lysis of contaminating erythrocytes. Neutrophils were $\geq 95\%$ pure as determined by Wright-Giemsa stain.

Statistical analyses. In Figures 5-7 and S5-S7, data represented as mean \pm s.e.m. Comparisons between two groups were assessed by the Student's *t* test (2 tail). A *p*-value of ≤ 0.05 was considered statistically significant.

SUPPLEMENTAL REFERENCES

- Anand, P., Brown, J.D., Lin, C.Y., Qi, J., Zhang, R., Artero, P.C., Alaiti, M.A., Bullard, J., Alazem, K., Margulies, K.B., *et al.* (2013). BET bromodomains mediate transcriptional pause release in heart failure. *Cell* *154*, 569-582.
- Anders, L., Guenther, M.G., Qi, J., Fan, Z.P., Marineau, J.J., Rahl, P.B., Loven, J., Sigova, A.A., Smith, W.B., Lee, T.I., *et al.* (2014). Genome-wide localization of small molecules. *Nature biotechnology* *32*, 92-96.
- Filippakopoulos, P., Qi, J., Picaud, S., Shen, Y., Smith, W.B., Fedorov, O., Morse, E.M., Keates, T., Hickman, T.T., Felletar, I., *et al.* (2010). Selective inhibition of BET bromodomains. *Nature* *468*, 1067-1073.
- Gerstein, M.B., Kundaje, A., Hariharan, M., Landt, S.G., Yan, K.K., Cheng, C., Mu, X.J., Khurana, E., Rozowsky, J., Alexander, R., *et al.* (2012). Architecture of the human regulatory network derived from ENCODE data. *Nature* *489*, 91-100.
- Hnisz, D., Abraham, B.J., Lee, T.I., Lau, A., Saint-Andre, V., Sigova, A.A., Hoke, H.A., and Young, R.A. (2013). Super-enhancers in the control of cell identity and disease. *Cell* *155*, 934-947.
- Kunsch, C., Ruben, S.M., and Rosen, C.A. (1992). Selection of optimal kappa B/Rel DNA-binding motifs: interaction of both subunits of NF-kappa B with DNA is required for transcriptional activation. *Mol Cell Biol* *12*, 4412-4421.
- Langmead, B., Trapnell, C., Pop, M., and Salzberg, S.L. (2009). Ultrafast and memory-efficient alignment of short DNA sequences to the human genome. *Genome Biol* *10*, R25.
- Lin, C.Y., Loven, J., Rahl, P.B., Paranal, R.M., Burge, C.B., Bradner, J.E., Lee, T.I., and Young, R.A. (2012). Transcriptional amplification in tumor cells with elevated c-Myc. *Cell* *151*, 56-67.
- Loven, J., Hoke, H.A., Lin, C.Y., Lau, A., Orlando, D.A., Vakoc, C.R., Bradner, J.E., Lee, T.I., and Young, R.A. (2013). Selective inhibition of tumor oncogenes by disruption of super-enhancers. *Cell* *153*, 320-334.
- Loven, J., Orlando, D.A., Sigova, A.A., Lin, C.Y., Rahl, P.B., Burge, C.B., Levens, D.L., Lee, T.I., and Young, R.A. (2012). Revisiting global gene expression analysis. *Cell* *151*, 476-482.
- Matys, V., Kel-Margoulis, O.V., Fricke, E., Liebich, I., Land, S., Barre-Dirrie, A., Reuter, I., Chekmenev, D., Krull, M., Hornischer, K., *et al.* (2006). TRANSFAC and its module TRANSCOMP: transcriptional gene regulation in eukaryotes. *Nucleic Acids Res* *34*, D108-110.
- Rahl, P.B., Lin, C.Y., Seila, A.C., Flynn, R.A., McCuine, S., Burge, C.B., Sharp, P.A., and Young, R.A. (2010). c-Myc regulates transcriptional pause release. *Cell* *141*, 432-445.
- Ramsey, S.A., Knijnenburg, T.A., Kennedy, K.A., Zak, D.E., Gilchrist, M., Gold, E.S., Johnson, C.D., Lampano, A.E., Litvak, V., Navarro, G., *et al.* (2010). Genome-wide histone acetylation data improve prediction of mammalian transcription factor binding sites. *Bioinformatics* *26*, 2071-2075.
- Shin, H., Liu, T., Manrai, A.K., and Liu, X.S. (2009). CEAS: cis-regulatory element annotation system. *Bioinformatics* *25*, 2605-2606.
- Whyte, W.A., Orlando, D.A., Hnisz, D., Abraham, B.J., Lin, C.Y., Kagey, M.H., Rahl, P.B., Lee, T.I., and Young, R.A. (2013). Master transcription factors and mediator establish super-enhancers at key cell identity genes. *Cell* *153*, 307-319.

Yang, L., Froio, R.M., Sciuto, T.E., Dvorak, A.M., Alon, R., and Luscinskas, F.W. (2005). ICAM-1 regulates neutrophil adhesion and transcellular migration of TNF-alpha-activated vascular endothelium under flow. *Blood* *106*, 584-592.

Zhang, Y., Liu, T., Meyer, C.A., Eeckhoute, J., Johnson, D.S., Bernstein, B.E., Nusbaum, C., Myers, R.M., Brown, M., Li, W., *et al.* (2008). Model-based analysis of ChIP-Seq (MACS). *Genome biology* *9*, R137.